Supporting Information

Intravenous Implantable Glucose/Dioxygen Biofuel Cell with Modified Flexible Carbon Fiber Electrodes

Fernanda C. P. F. Sales, Rodrigo M. Iost, Marccus V. A. Martins, Maria C. Almeida,
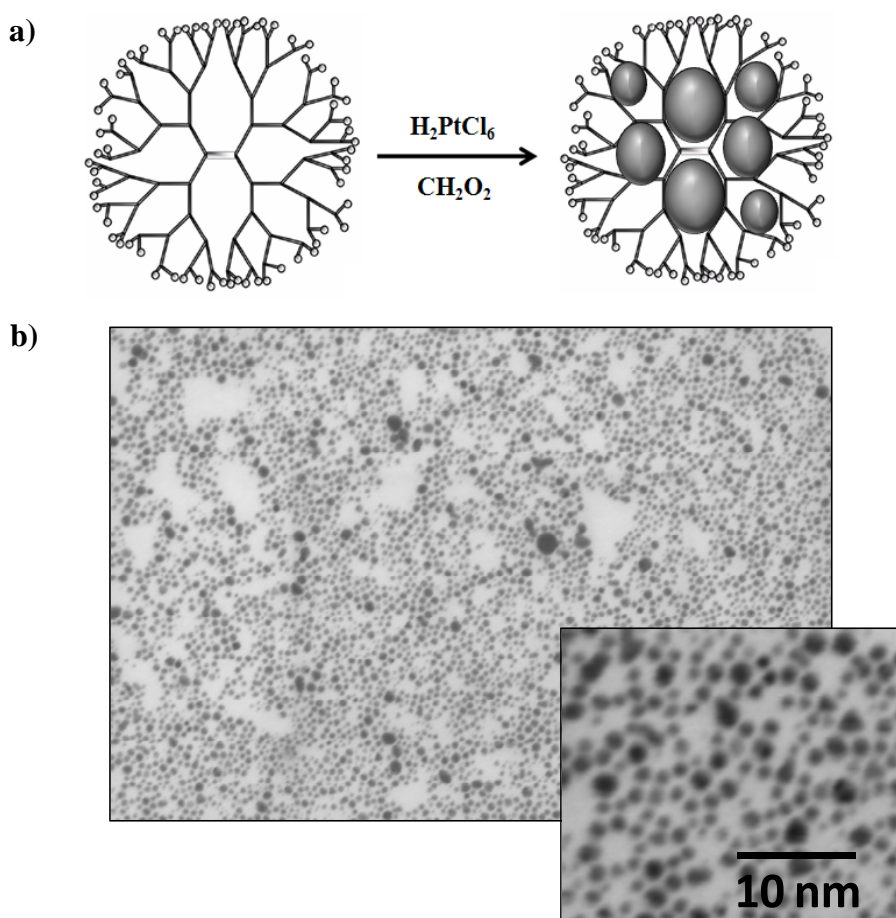*Frank N. Crespilho*

1 Synthesis of PAMAM-PtNP

a)

b)

10 nm

Figure S1. **a)** The synthesis of PAMAM-PtNP was carried out according to the following procedure: 1 mL of PAMAM-G4 dendrimer (1 mmol L^{-1}) was mixed with 1mL of precursor HPtCl$_4$ (1 mmol L^{-1}). **b)** TEM images of PAMAM-PtNP with average size of 3 nm.

2 Bioanode Composition

The surface composition of the modified electrodes was determined by using two different methods. Firstly, we have carried out chronoamperometry in order to determine the charge of NR, and consequently, the amount of NR per area the electrode. The second, the density of enzyme were determined by using UV-VIS spectroscopy. Also, the thickness of the bio-film deposited onto the carbon fiber was measured by using AFM in the contact mode. All the experimental details and the result is show in following.

2.1 Surface composition: Neutral red

The determination of NR surface composition was carried out by immersing FCF microelectrodes onto a solution and the quantity of NR were quantified upon application of 0.4V using chronoamperometry. Figure S2 shows a scheme of the experimental modification of FCF microelectrodes with NR solution 0.16 mmol L^{-1}.
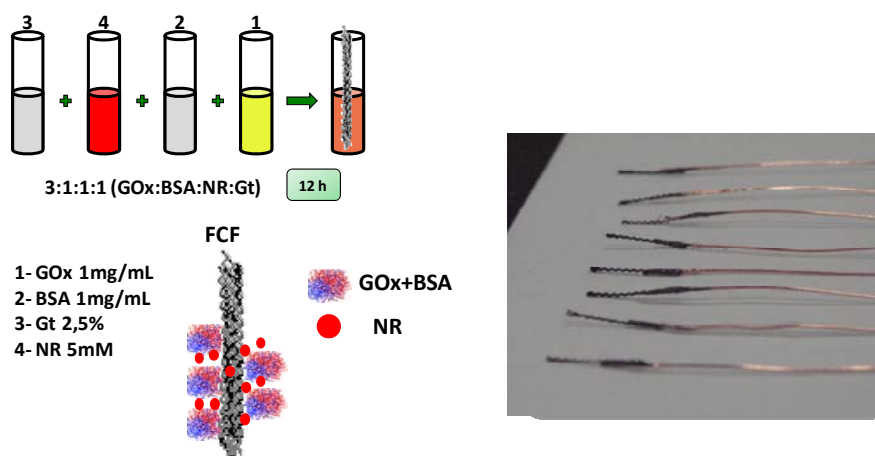

3:1:1:1 (GOx:BSA:NR:Gt)   12 h

FCF

1- GOx 1mg/mL
2- BSA 1mg/mL
3- Gt 2,5%
4- NR 5mM

GOx+BSA

NR

Figure S2. Scheme of FCF modified electrodes with NR redox mediator 0.16 mmol L^{-1} solution adsorbed upon 12 hours of immersion.

Figure S3 shows the chronoamperometry results obtained for FCF microelectrodes upon applied potential of 0.4V. The results were achieved using three different FCF modified microelectrodes indicated by 1,2 and 3 with the aim intent to verify the reproducibility of experiments. Also, the integration of all the chronoamperograms are also showed in figure 4 and also the electrochemical reaction of NR redox mediator at pH = 7.2. All the electrochemical experiments were carried out using a potentiostat/galvanostat AUT84223, Autolab.
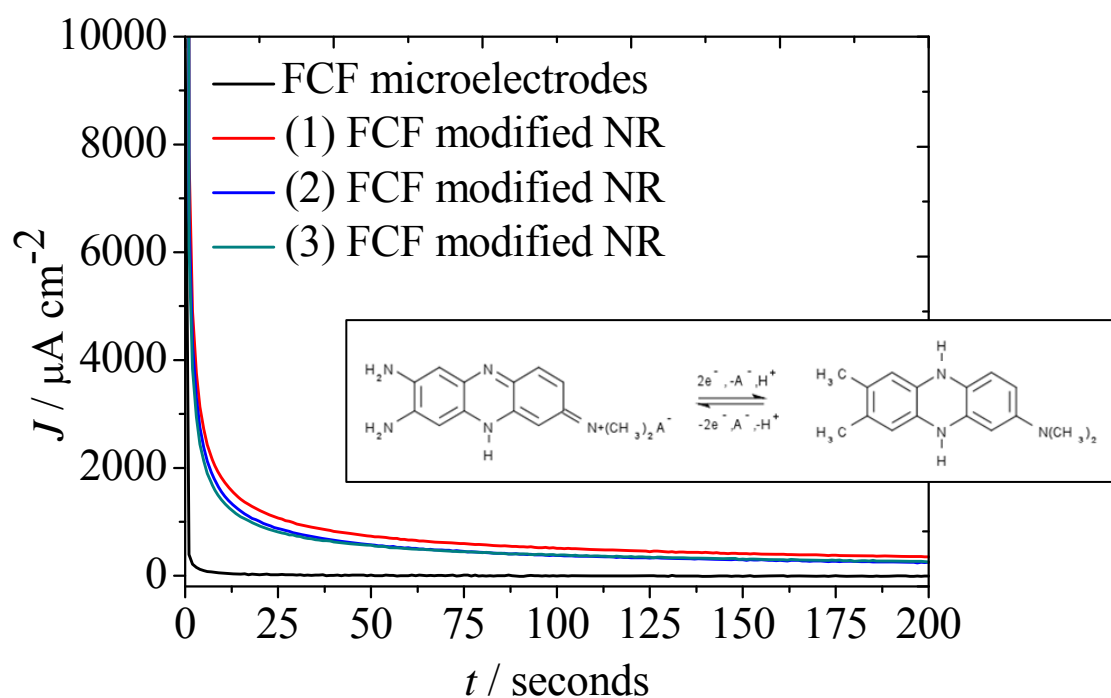
Figure S3. Chronoamperometry of FCF microelectrode and FCF modified microelectrodes after adsorption of NR upon 12 hours of adsorption. Applied potential: 0.40 V. Electrolyte support: PBS 0.1 mol L^{-1} (pH = 7.2).

The amount of NR adsorbed on FCF microelectrodes were determined by integration of chronoamperograms. Thus, we have the correlation of charge density dependence with square root of time:

$$Q = \int_{t=0}^{t} j(t)dt = \int_{t=0}^{t} \frac{nFAC_{NR}D^{1/2}}{\pi^{1/2}t^{1/2}} = kt^{1/2}$$

where Q is the charge associate with the adsorbed NR at FCF microelectrode, F the Faraday constant, t the time course (seconds), n the numbers of electrons, C_{NR} the NR redox mediator concentration, k the electron transfer constant, A the electrode area and D the diffusion constant of ionic species presents at electrolyte solution. The charge obtained is listened in table S1 for each FCF microelectrode with the corresponding mol

of electrons ($Q = ne$). For each electrode we select similar carbon fiber with the same electrode length.

Table S1. Parameter obtained from integration of chronoamperograms (in triplicate).

Electrodes	Q (C cm^{-2})	Electrons (mol)	Mass of NR $_{adsorbed}$
1	2.0854×10^{-5}	0.6516×10^{14}	15.6 ng cm^{-2}
2	1.5939×10^{-5}	0.4981×10^{14}	11.9 ng cm^{-2}
3	1.6992×10^{-5}	0.531×10^{14}	12.7 ng cm^{-2}

The results obtained show the mass of NR per FCF electrode area (ng cm^{-2}). The three electrodes (triplicate experiments) showed similar mass of NR adsorbed onto FCF electrode, with average mass of adsorbed NR of $\overline{m}$ = 13.4 ng cm^{-2}.

2.2 Surface composition: Density of enzyme

The surface charge of GOx-BSA was determined using an UV-Vis spectroscopy. Enzyme GOx shows two well-defined bands at visible range at around 378 nm and 420 nm associated with prosthetic group FAD and the absorption of these bands were used to determine the mass of enzyme GOx adsorbed onto FCF microelectrodes. For this purpose, 70 FCF microelectrodes (length of 1.20 ± 0.05 mm for each FCF) were immersed in a mixture of GOx (1mg mL^{-1}), BSA (1.0 mg mL^{-1}), GA (2.5%) and NR redox mediator (1.0 mmol L^{-1}) in the proportion 3:1:1:1 (v/v) with total solution mixture volume of 2.0 mL. The electronic spectra of the resulting mixture solution were measured before and after immersion of FCF microelectrodes. After 12 hours of immersion, FCF modified microelectrodes were removed from the solution and the absorption of the resulting solution were recorded. The electronic spectra at ultraviolet/visible (UV-VIS) range were performed utilizing spectrophotometer V-670 spectrophotometer JASCO in the range of 190 to 800 nm. The mass of FCF microelectrodes were measured using a mass-balance Adventure, model AR2140BR (±0.0001 g).

Figure S4 exhibit the UV-Vis spectra for GA (0.42%), BSA (0.17 mg mL^{-1}), GOx (0.5 mg mL^{-1}) and mixture of the solutions (GA + GOx + BSA). GOx shows two absorption bands at about 380 and 450 nm in PBS, which is the characteristic absorption

of oxidized FAD group. In mixture of the solutions (GA + GOx +BSA), the absorption bands of GOx occur at the same wavelengths.
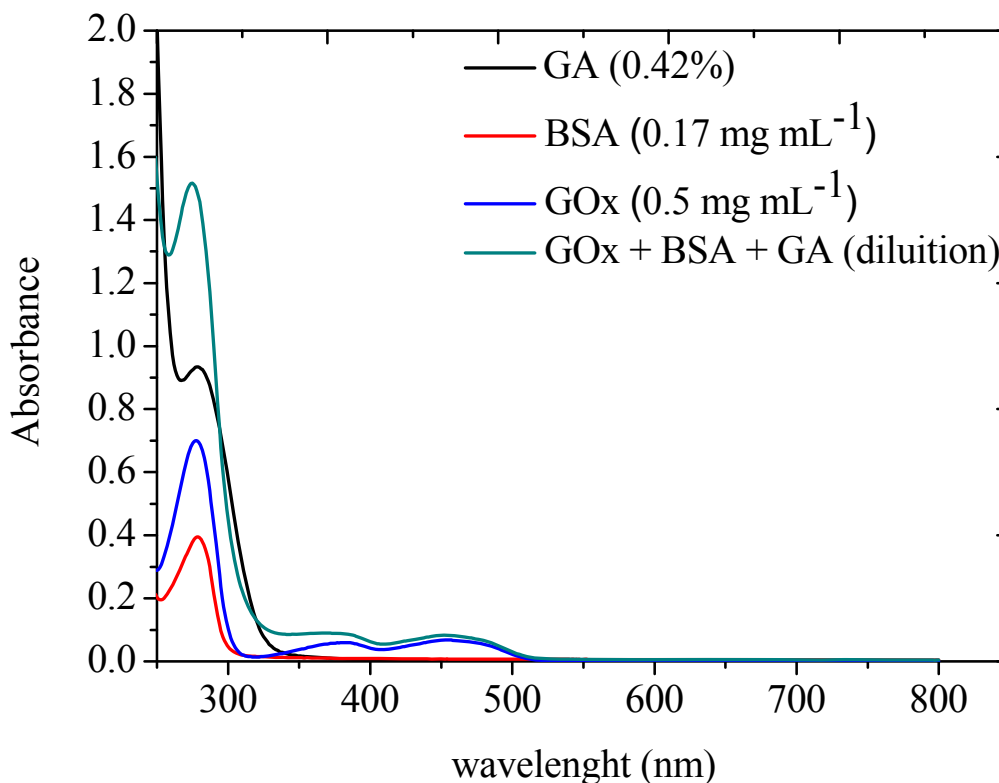

Figure S4. Electronic spectroscopy in the UV-Vis range of GA (0.42%)(black line), BSA (0.17 mg mL^{-1})(red line), GOx (0.5 mg mL^{-1}) and mixture of the solutions (GA + GOx + BSA)(green line). All the solution were prepared in PBS 0.1 mol L^{-1} (pH = 7.2).

Figures S5 and S6 show UV-Vis absorption spectra of the mixture GOx, GA and BSA in different dilution. Based in this result, we have obtained calibration curve for GOx (variation of absorbance at λ = 451 nm *versus* enzyme GOx concentration) and it was calculated the concentration of enzyme GOx absorbed in fiber microelectrodes. In terms of the solution, the results was 0.884 mg mL^{-1} in resulting solution and 0.116 mg mL^{-1} for absorbed on electrode surface. This result leading to enzyme loading:

- 18.8 mg$_{(enzyme)}$ g^{-1}$_{(FCF\ electrode)}$

- 18.8 mg of GOx enzyme corresponding to 1.1 x 10^{19} Dalton

- 7.06 x 10^{13} molecules that corresponding to 0.11 nmol g^{-1}

- The final bioanode composition corresponding to 38.5 fmol of GOx per microelectrode used.
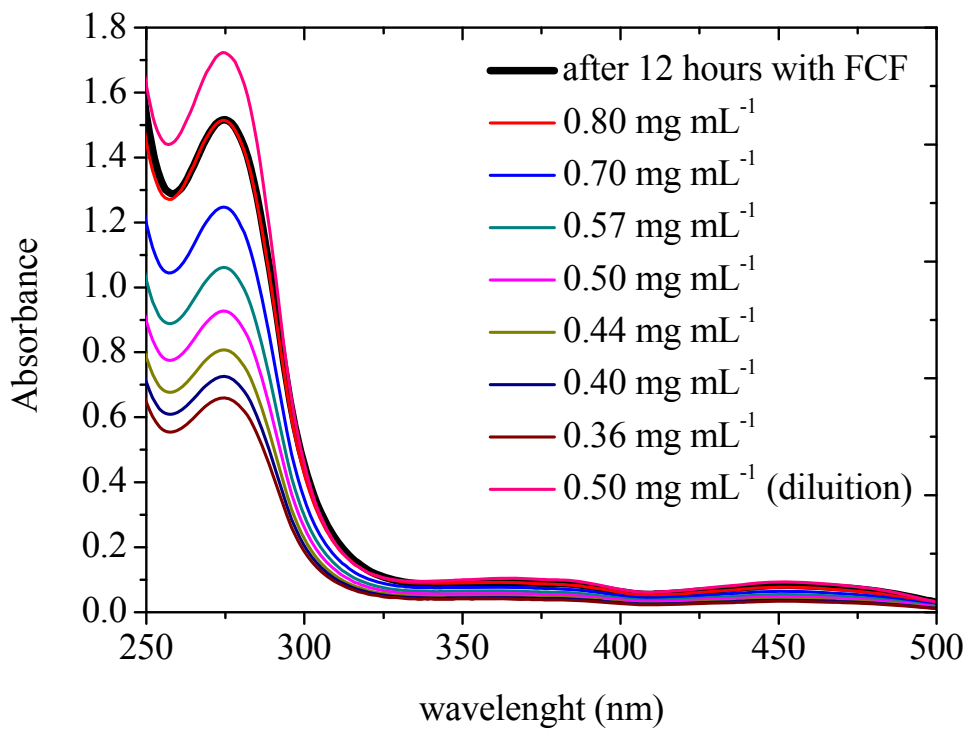

Figure S5. UV-Vis spectra for dilution of (GOx + BSA + GA) solution and the electronic spectra of the same solution after the immersion of FCF microelectrodes during 12 hours (black line). All the solution were prepared in PBS 0.1 mol L^{-1} (pH = 7.2).
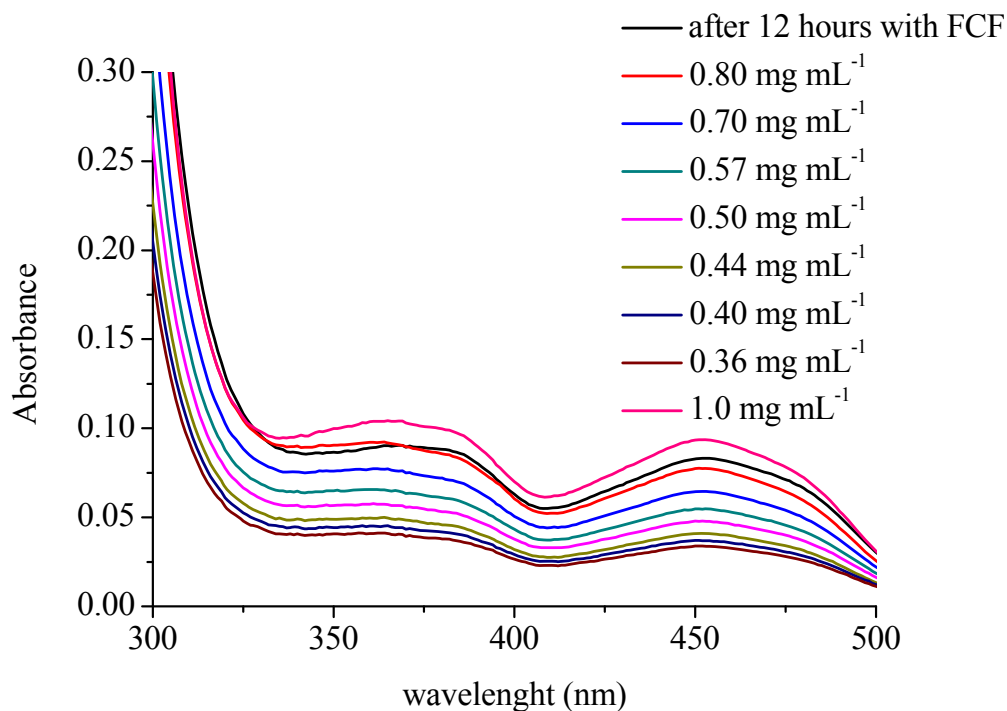
Figure S6. Zoomed UV-Vis spectra of figure S5. All the solution were prepared in PBS 0.1 mol L^{-1} (pH = 7.2).
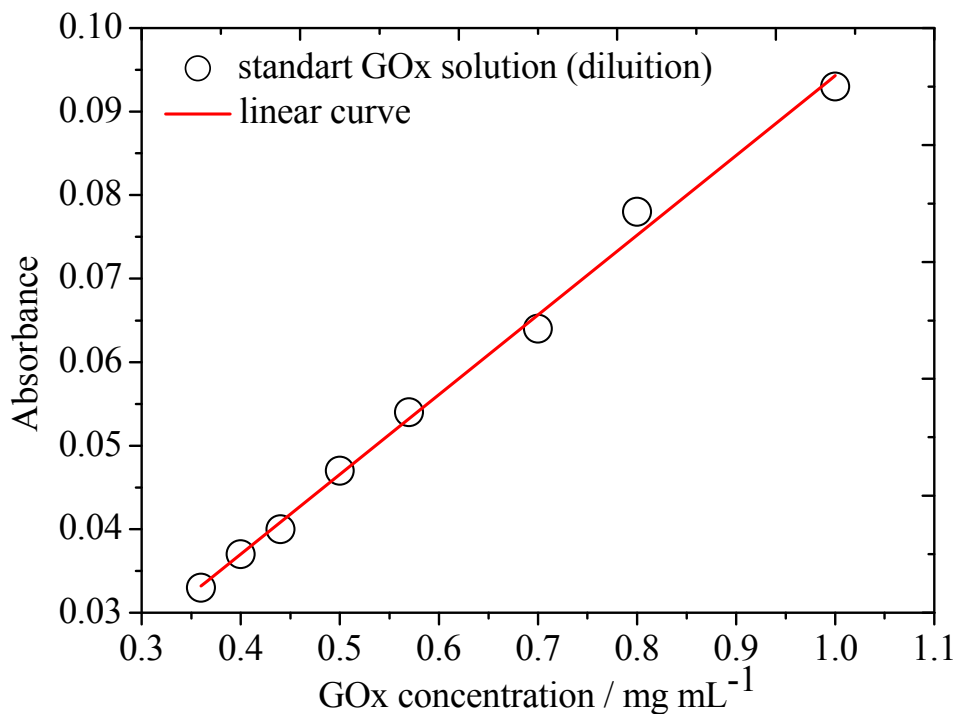

Figure S7. Absorbance *versus* GOx concentration in PBS 0.1 mol L^{-1} (pH = 7.2). The absorbance values was obtained at $\lambda = 451$ nm.
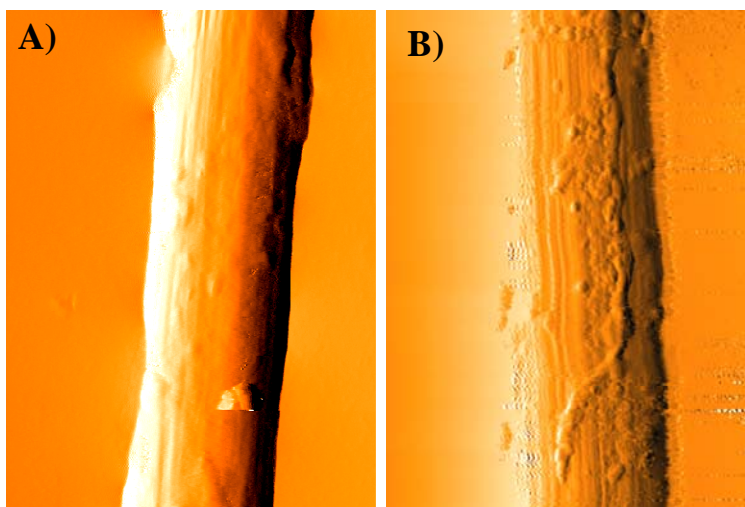
2.3 Bio-film thickness on FCF electrode

Figure S8. **A)** FCF microelectrode before modification and **B)** after modification of FCF microelectrodes with GOx-BSA film.

The images showed clearly the presence of the GOx-BSA film adsorbed onto FCF microelectrodes surface. We can observe a more flat surface before modification with enzyme and the increase in roughness of FCF surface after GOx-BSA immobilization (figure S8B). This results show a good information about the presence of GOx-BSA film onto FCF surface with increase of roughness from 11.2 nm for FCF to 160.54 nm for FCF modified with GOx-BSA film.

Further information was obtained about the thickness of the film formed onto FCF microelectrode surface as showed in figure S9. After adsorption (red line), the GOx-BSA film showed a thickness around 70 nm. The obtained thickness determination was conducted by two ways: (i) the difference in the thickness at the top and (ii) at the region pass throughout transversal region of glassy substrate and FCF microelectrode deposited previously (Figure S9). For the two paths, GOx-BSA thickness showed the same value at around 70 nm and the same procedure were realized in different locations of the unmodified and modified region of the FCF microelectrodes.
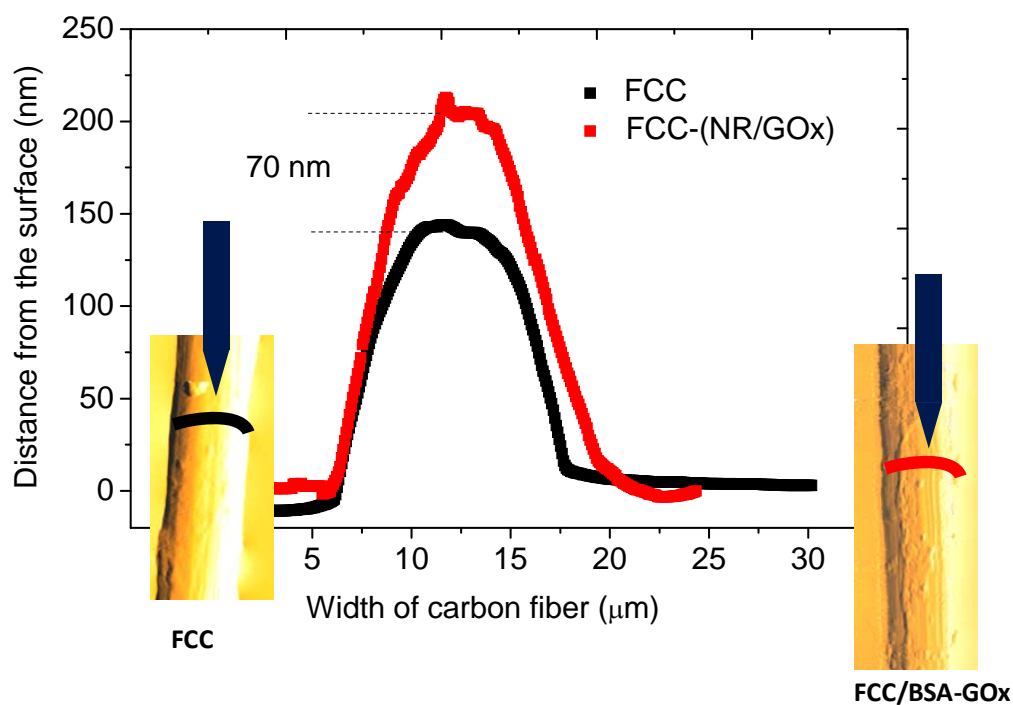
Figure S9. FCF (black line) shows an increase of 70 nm in height after modification with GOx-BSA (red line).

3 PAMAM-PtNPs hybrids as electrocatalysts

Regards the use of PAMAM-PtNPs hybrids as electrocatalysts components for cathodes, there is some studies in literature that show their potential application due to PAMAM-PtNPs not hind the diffusion of oxygen [reference 4 in the paper]. This feature was clearly evidenced by the increase in the electroreduction current density. To support this affirmation, a comparative study using platinum microwire of the same dimensions (light gray) and FCF modified with PAMAM-PtNPs (black) was take place, as shown in figure 2. The same experimental conditions were used for the two electrode configuration. The results shows the high current density obtained compared to platinum wire of the same dimensions. High current densities is observed for FCF-PAMAM-PtNPs when compared with microwire.
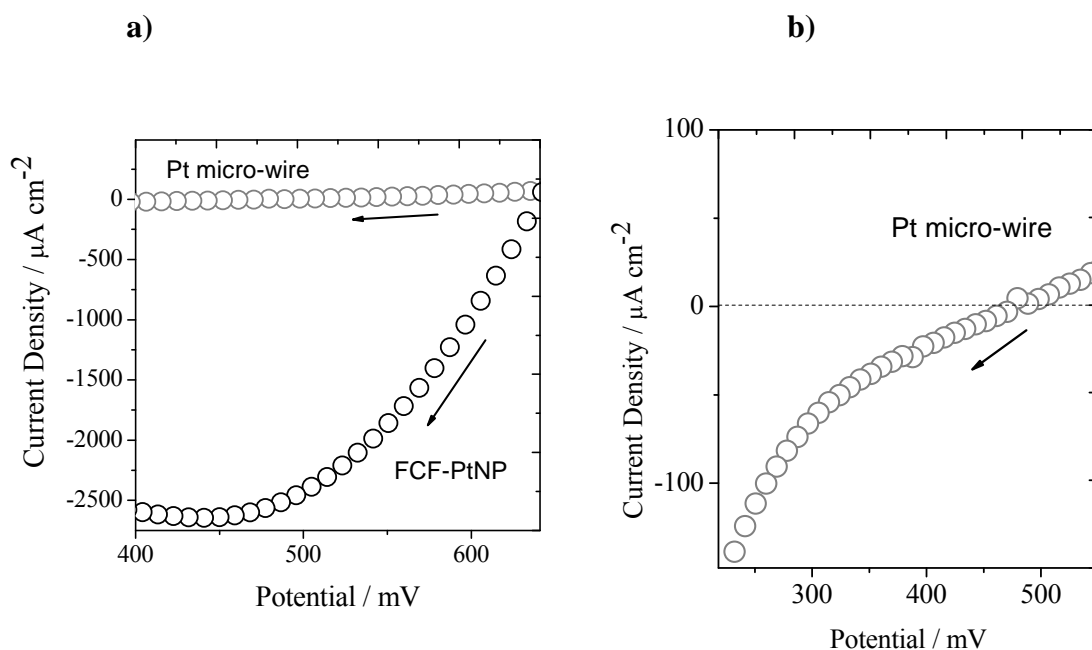
a)   b)

Figure S10. **a)** Linear voltammetry obtained for using platinum microwire with the same dimensions (light gray) of FCF modified with PAMAM-PtNPs (black) in the presence of O_2. Scan rate: 10 mV s^{-1}. Supporting electrolyte: PBS (50.0 mmol L^{-1}, pH = 7.2). **b)** zoomed region for Pt micro-wire.

A comparative result was also obtained for the case of the glassy carbon electrode (GC) with PAMAM-PtNPs (GC-PAMAM-PtNPs) (*Figure S11*). One more time, it can see the high current density for FCF-PAMAM-PtNPs. These results shows the contribution of the FCF electrode used here, in order to improve the oxygen reduction, and also for the performance of the implanted BFC reported here.
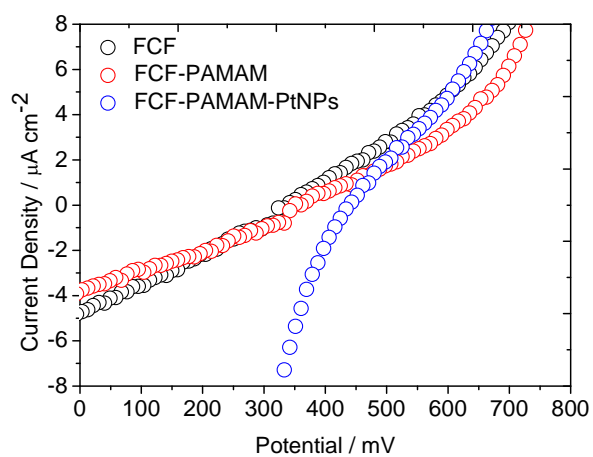
a)
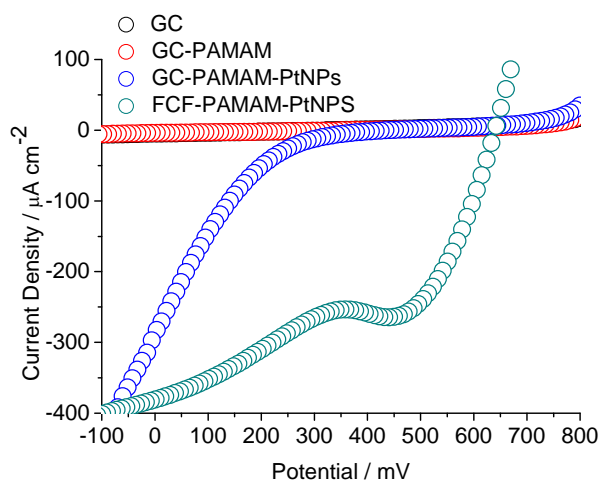
b)

Figure S11. **a)** Linear voltammetry obtained for GC electrode (black), GC-PAMAM (red), GC-PAMAM-PtNPs (blue**)** and FCF-PAMAM-PtNPs with dissolved O_2. **b)** Zoomed region. Scan rate: 10 mV s^{-1}. Supporting electrolyte: PBS (50.0 mmol L^{-1}).

4 Important parameters that can lead to losses power output

Membrane : In the case of this work, the membrane was not used due to the size of the micro-device developed here. We have tried to use Nafion® membranes (several thickness), but the BFC doesn't work well.

Glucose oxidation at the cathode: Oxidation of glucose at cathode can occur, as showed by linear voltammograms in figure S12, when FCF/PAMAM-PtNPs was used in the presence of glucose 47 mmol L^{-1}. In presence of glucose, the current for reduction O_2 decrease, but the electrode still working.
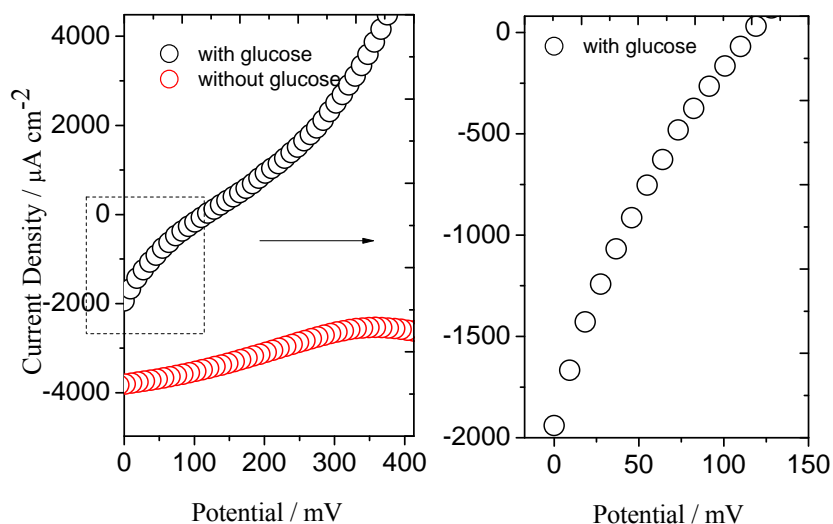

Figure S12. Linear voltammetry obtained for FCF-PAMAM-PtNPs in the presence and in absence of glucose 47 mmol L^{-1}. Scan rate: 10 mV s^{-1}. Supporting electrolyte: PBS (50.0 mmol L^{-1}, pH = 7.2).

Oxygen compete with NR: As expected, the oxygen compete with NR, as showed in figure S13. However, it is clearly appears that even in the presence of oxygen the biocathode still oxidizing glucose near to the thermodynamic potential of the enzyme-mediator. Also, it is observed that in the absence of NR, negative currents indicates that there is oxygen reduction (with possible formation of hydrogen peroxide) current more pronounced than glucose oxidation current. This fact confirms that NR is very important as mediator in these electrodes.
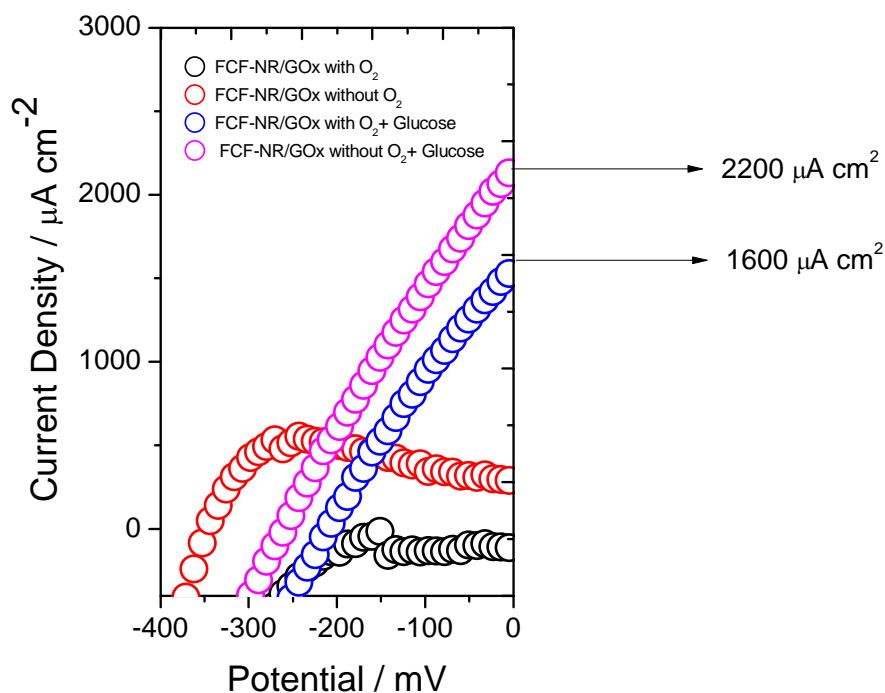
Figure S13. Linear voltammetry for different electrodes configuration in the presence and in absence of glucose 47 mmol L^{-1} and saturated dioxygen. Scan rate: 10 mV s^{-1}. Supporting electrolyte: PBS (50.0 mmol L^{-1}, pH = 7.2).

4 Long-term Stability

The Figure S14 shows Long-term stability for the power density of the intravenous implantable BFC up to 24 hours. Regarding to stability, all experiments were performed in 24 hours (time of the effect of anesthesia on the animal). It was observed that the power output begins at 180 μW cm^{-2} and decrease to 95 μW cm^{-2} with 5 minutes of experiment. Then, with some fluctuation, the power is stabilized about 100 μW cm^{-2} for 24 hours.
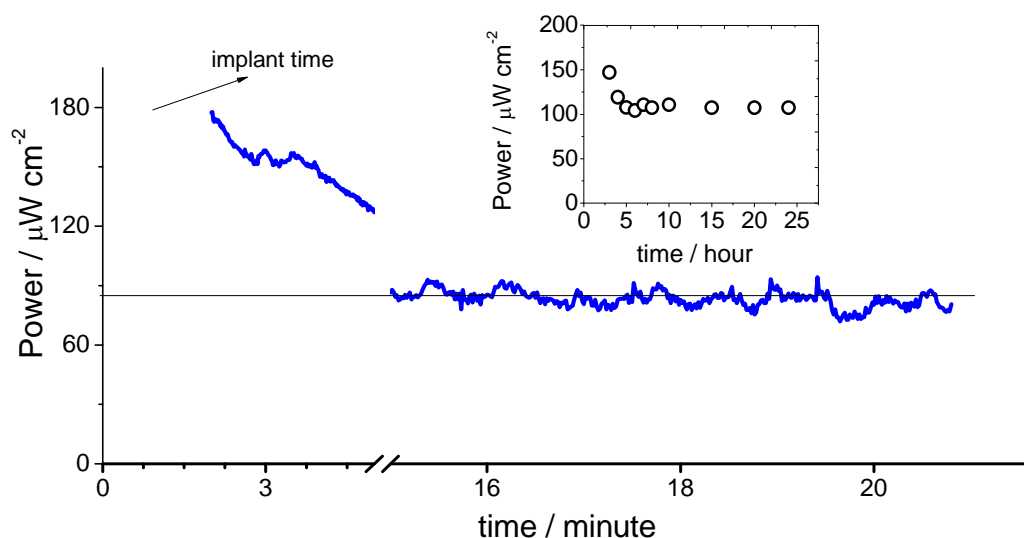
Figure S14. Long-term stability for the power density of the intravenous implantable BFC up to 24 hours. Regarding to stability, all experiments were performed in 24 hours (time of the effect of anesthesia on the animal). It was observed that the power output begins at 180 µW cm^{-2} and decrease to 100 µW cm^{-2} with 5 minutes of experiment. Then, with some fluctuation, the power is stabilized about 100 µW cm^{-2} for 24 hours.

5 Equations for the electrochemical parameters

In order to compare the performance of the BFCs in the *in vitro* and *in vivo* experiments, we evaluated the electrochemical parameters involved in the catalytic process. We considered 4 cases: (1) The theoretical thermodynamic parameters of cathodic and anodic reactions were based on Gibbs free energy. (2) The theoretical thermodynamic parameters (not in equilibrium) were obtained for a half-cell through *in vitro* experiments. (3) The electrochemical parameters were obtained for a BFC operating *in vitro*. (4) The electrochemical parameters were obtained for a BFC operating *in vivo*. For case 1, the free energy can be obtained by using the standard potential required for oxygen reduction and glucose oxidation. The glucose/O$_2$ BFC generates electricity only if the overall reaction is thermodynamically favorable; in this case, both the reactions are favorable. The electrochemical reactions can be evaluated in terms of the Gibbs free energy expressed in Joules (J), and the maximum work derived and the cell electromotive force from the 2 semi-reactions can be calculated as follows.

$$\Delta G_r = \Delta G_r^0 + RT \ln(Q) \qquad (2)$$

$$E_{emf} = E_{emf}^{0} - (RT/nF) \ln(Q) \qquad (3)$$

where ΔG_r (J) is the Gibbs free energy under specific conditions, ΔG_r^0 (J) is the Gibbs energy under standard conditions (298.15 K, 1 bar pressure, species concentration 1.0 molL^{-1}), R (8.31447 J mol^{-1} K^{-1}) is the universal gas constant, T (K) is the absolute temperature, Q is the reaction quotient (activities of products divided by those of reactants), and E^0_{emf} (V) is the standard cell electromotive force. Table 1 summarizes the values of electrochemical parameters of the FCF-NR/GOx‖FCF-PAMAM-PtNP BFC.

From the results obtained for the implantable BFC operating *in vivo* and the experimental results for the half-cells used *in vitro*, we inferred that other variables should also be considered, for instance, internal voltage losses. The theoretical parameters obtained from the half-cells included the potential at zero-current values of the cathode and the anode, and the OCV values of the BFC with the final configuration were theoretically estimated. The electrical energy generated by anodic/cathodic reactions via electrochemical processes is commonly measured as the power generated per area or volume of the electrochemical cell (*C. M. A. Brett and A. M. O. Brett, Electrochemistry principles, methods, and applications, Oxford New York Oxford University Press, New York, 1993.; A. J. Bard and L. R. Faulkner, Electrochemical Methods: Fundamentals and Aplications, 2 edn., John Wiley, New Jersey, 2000*). The theoretical cell voltage can be obtained using equation 4.

$$E_{Cell} = E_C - E_A - \Sigma IR_e \qquad (4)$$

where E_{Cell} denotes the potential of the liquid electrolyte and E_C and E_A represent the potential of the cathode and anode, respectively. ΣIR_e denotes the total internal voltage loss of the electrochemical cell. The standard potential for a BFC can be obtained from the semi-reactions in a half-cell, as given by the Nernst equation (5).

$$E_{Cell} = E_e^{0} + \frac{RT}{nF} \log\left(\frac{[Ox]}{[Red]}\right) \qquad (5)$$

E_{Cell} can be estimated from the current generated by the electrochemical reactions. In this case, the residual potential $E_{Cell} = E_C - E_A - \Sigma IR$ is given as follows (6)

$$\eta = E - E_e \tag{6}$$

where E_e corresponds to the equilibrium potential of the electrode. The current density generated in an electrochemical cell can be optimized by minimizing the ohmic resistance (ΣIR_e).